Dynamical Climatology

Nuclear Winter: Calculations of the shortwave radiative effects of soot aerosols.

by

A. Slingo and P. Goldsmith

DCTN 24 May 1985

Meteorological Office (Met. O. 20)
London Road
Bracknell
Berkshire RG12 2SZ

DYNAMICAL CLIMATOLOGY TECHNICAL NOTE. 24

NUCLEAR WINTER: CALCULATIONS OF THE SHORTWAVE RADIATIVE EFFECTS OF SOOT AEROSOLS

by

A Slingo and P Goldsmith

Submitted as a letter to Nature

Met O 20 (Dynamical
Climatology Branch)
Meteorological Office
London Road
Bracknell
Berkshire, U.K. RG12 2SZ

May 1985

Note: This paper has not been published. Permission to quote from it should be obtained from the Assistant Director of the above Meteorological Office Branch.

Nuclear Winter: Calculations of the Shortwave Radiative Effects of Soot Aerosols

A Slingo and P Goldsmith

Meteorological Office, London Road, Bracknell, Berkshire, RG12 2SZ, England

Several studies have appeared recently of the climatic consequences of atmospheric aerosols generated by a nuclear war[1-5]. All ignore the wavelength-dependence of the interaction between the aerosol and solar (shortwave) radiation, taking scattering data for a single wavelength (usually 0.55μm) to be representative of the entire solar spectrum. Results from a spectrally-detailed radiation scheme demonstrate that this assumption overestimates the impact of the aerosol, by a factor which increases with the aerosol mass loading. The calculations also emphasize the extreme sensitivity of the magnitude of the radiative perturbation to the aerosol size, refractive index and loading. They support the concept of a threshold loading, below which the aerosol would be expected to warm the surface rather than cool it. It is suggested that much more work is needed using 3-D models to study the impact of a wide range of aerosol loadings and of the induced circulation changes. The effects of soot aerosols on solar radiation could be included in such models by assuming simple exponential absorption with an attenuation coefficient of about 1.5 m^2g^{-1}.

Calculations have been performed with a detailed solar radiation scheme[6] which has been employed previously in a wide range of studies[7-10]. It uses 24 spectral bands in the wavelength range 0.2-4 μm to model the transfer of solar radiation through the atmosphere. The effects of scattering are included through the Delta-Eddington approximation[11] and of the interaction between scattering and gaseous absorption by the Exponential Sum Fitting of Transmissions technique[12].

The aerosol considered here is the smoke generated by post-nuclear fires[2], whose density is assumed to be 1 g cm^{-3} [1,2]. The real and imaginary parts of the refractive index were interpolated from published data for soot[13] (as used in some previous studies[1,2]) to the nominal central wavelengths of each spectral band of the radiation scheme. The refractive index increases from about 1.75-0.44i in the visible region of the spectrum to 1.92-0.58i at 4 μm wavelength. On the assumption that the particles are spherical with a log-normal radius distribution[14], their single scattering properties were calculated using Mie theory[15]. The assumption of sphericity is of course a gross one but is used here to enable illustrative calculations to be made.A very narrow size distribution was used at first (variance of the logarithms of the radii[14] = 0.001) in order to demonstrate the strong dependence on the aerosol size. The calculated specific extinction coefficient and $1-\tilde{\omega}$ (where $\tilde{\omega}$ is the single scattering albedo[15]) are plotted on Figure 1 as a function of the wavelength of the incident radiation for various values of geometric mean radius[14]. The curves illustrate many of the well known properties of the Mie solutions[15] as a function of the size parameter $x = 2\pi r/\lambda$, from large-particle approximations ($x>>1$) to Rayleigh scattering ($x<<1$). Of

importance here is the strong dependence on both the aerosol radius and the wavelength. Previous studies[1-5] have ignored the wavelength dependence, using representative values for 0.55 μm or 0.7 μm [2] instead.

These data were used as input to the radiation scheme to calculate the spectral distribution of the upward and downward fluxes in a Mid-Latitude Summer atmosphere[16]. The scheme was run with a vertical resolution of 1 km from the surface up to 25 km,with a coarser grid thereafter to 100 km altitude. The aerosol mass per unit volume was constant from the surface up to 12 km. This is a convenient assumption for the present study, although the climatic response is known to be sensitive to the aerosol vertical distribution[17]. At each level and in each spectral band the effects of absorption by water vapour and ozone, Rayleigh scattering and aerosol scattering and absorption were included, but clouds were ignored. The surface albedo was 0.2 at all wavelengths. Figure 2 shows the downward shortwave flux at the surface as a function of the aerosol loading and mean radius, for a solar zenith angle of 60°. Similar results were obtained with zenith angles of 30° and 75°. The attenuation is practically independent of radius for the smallest particles, rising to a maximum at about 0.1-0.2 μm and thereafter decreasing rapidly. This behaviour is to be expected from Figure 1.

It is important to estimate the effect of using the aerosol single scattering properties at 0.55 μm wavelength to calculate the broad-band fluxes, as in previous studies[1-5]. This was done by scaling up the fluxes from the scheme for this wavelength, to give the dashed lines on Figure 2. For the largest aerosols, the properties at 0.55 μm give a good

estimate of the broad band fluxes, because of the weak wavelength dependence shown on Figure 1. Below 0.5 μm radius, however, the aerosol attenuation is over-estimated because this simple approach fails to account for the rapid decrease in the specific extinction coefficient with increasing wavelength, which allows a much larger fraction of the near-infrared radiation to reach the surface. For the higher aerosol loadings, the over-estimate is equivalent to using an aerosol loading which is at least a factor of 2 too large.

In the recent report from the US National Academy of Sciences[5] (NAS), the baseline calculations assume a lower smoke refractive index than used above (1.55–0.1i at 0.55 μm) and a broader, more realistic, size distribution (mean radius 0.1 μm, logarithmic variance 0.48045). The effect of these differences will be examined in turn. The single scattering data for the narrow size distribution and mean radius 0.1 μm, but with the NAS refractive index at all wavelengths, are shown as the dashed curves labelled 0.1* on Figure 1. Comparison with the solid curve labelled 0.1 shows that the lower refractive index leads to much smaller extinction coefficients and that both these and $1-\tilde{\omega}$ have a slightly stronger wavelength dependence. As a result, the downward flux at the surface is considerably larger for a given aerosol column density and the error associated with ignoring the wavelength dependence is also enhanced (Figure 3).

The curves labelled NAS on Figures 1 and 3 were obtained with both the lower refractive index and the broader size distribution and thus correspond exactly to the NAS baseline aerosol properties. Comparison of

the two pairs of dashed lines on Figure 1 shows that broadening the size distribution reduces the wavelength dependence of the data, because of enhanced contributions from the larger aerosols. The impact on the broad band fluxes is small (Figure 3), but the error from ignoring the wavelength dependence is reduced. Nevertheless, the error is still significant, corresponding to the use of an aerosol loading which is about 50% too large at the highest loadings considered here. Such an error could lead to an overestimate of the surface temperature reduction by as much as 10°C[18].

Vertical profiles of the atmospheric heating rates for the NAS baseline aerosol properties are plotted on Figure 4. For the largest aerosol loadings there is strong heating of the top of the smoke cloud and surface cooling (compared with the clear-sky case). For the smallest loadings the perturbation is very small and could not induce significant surface cooling. Indeed, one would expect the surface to be warmed compared with the no-aerosol case, because convection would still occur and so the aerosol heating would be shared between the atmosphere and surface[18]. That heating of both components of the surface-atmosphere system would occur is demonstrated by the drop in the value of the reflected flux at the top of the atmosphere (inset table on Figure 4). As the aerosol loading increases, however, convection would be suppressed and the "classic" nuclear winter response of a heated atmosphere decoupled from a cooled surface would result.

A proper assessment of the likelihood of nuclear winter therefore requires a determination of the threshold loading[18] which marks the transition between the surface heating and cooling regimes. One-dimensional

models can at best only give qualitative guidance because of the patchy nature of the smoke cloud. Three-dimensional general circulation models with interactive aerosol transport are required to study global aspects of the climatic response to various aerosol loadings. Nevertheless, in such models important processes such as coagulation, washout and motions on a wide range of unresolved scales will either be ignored or crudely parametrized. Credible modelling of these effects requires the use of detailed cloud- and meso-scale models which must also include adequate formulations of radiative processes. The results shown here suggest that the effects of smoke aerosols on solar radiation could be included very simply in any of the above models because, for example, the NAS data plotted on Figure 3 can be fitted to a reasonable approximation by assuming simple exponential attenuation of the incoming solar radiation at the top of the aerosol layer with a specific extinction coefficient of 1.5 m^2g^{-1}. Results (not shown here), similar to those in Figure 4 but for different aerosol vertical distributions, indicate that such a simple formulation can also represent the vertical profile of atmospheric heating. A wide range of existing numerical models could thus be brought to bear on the nuclear winter problem with minimal changes.

References

1. Turco R.P., Toon O.B., Ackerman T.P., Pollack J.B. and Sagan C., Science, 222, 1283-1292 (1983)

2. Crutzen P.J., Galbally I.E. and Brühl C., Climatic Change, 6, 323-364 (1984).

3. Covey C., Schneider S.H. and Thompson S.L., Nature, 308, 21-25 (1984).

4. Aleksandrov V.V. and Stenchikov G.L., in Proceedings on Applied Mathematics, (Moscow, 1983).

5. The effects on the atmosphere of a major nuclear exchange, National Academy of Sciences (Washington, 1985)

6. Slingo A. and Schrecker H.M., Quart. J.R. Met. Soc., 108, 407-426 (1982)

7, Slingo A., Nicholls S. and Schmetz J., Quart. J.R. Met. Soc., 108, 833-856 (1982)

8. Herman G.F. and Curry J.A., J.Clim. Appl. Met., 23, 5-24 (1984)

9. Shine K.P., Quart. J.R. Met. Soc., 110, 747-764 (1984)

10. Shine K.P., Henderson-Sellers A. and Slingo A., Quart. J.R. Met. Soc., 110, 1170-1179 (1984)

11. Joseph J.H., Wiscombe W.J. and Weinman J.A., J.Atmos. Sci., 33, 2452-2459 (1976)

12. Wiscombe W.J. and Evans J.W., J.Comp. Phys. 24, 416-444 (1977)

13. Shettle E.P. and Fenn R.W., Environmental Research Paper No.676, (Air Force Geophysics Laboratory, Massachusetts, USA, 1979)

14. Fuchs N.A., The mechanics of aerosols (Pergamon, 1964)

15. Twomey S., Atmospheric Aerosols (Elsevier, Amsterdam, 1977)

16. McClatchey R.A., Fenn R.W., Selby J.E.A., Volz F.E. and Garing J.S., Environmental Research Paper No. 411, (Air Force Cambridge Research Laboratories, Massachusetts, USA, 1972)

17. Ramaswamy V. and Kiehl J. T. Submitted to J. Geophys. Res. (1984).

18. Cess R. D., Potter G. L. and Gates W.L. Preprints of Third Conference on Climatic Variations, American Meteorological Society, Los Angeles, 7-11 January 1985.

Figure Captions

Fig. 1. Specific extinction coefficient ($m^2\ g^{-1}$) and $1-\tilde{\omega}$ (where $\tilde{\omega}$ is the single scattering albedo) as a function of the wavelength λ of the incident radiation, for spherical soot aerosols with a very narrow size distribution and various values of the geometric-mean radius r_g from 0.01 μm to 1.0 μm (solid lines). For the dashed lines labelled 0.1* the refractive index was changed to 1.55-0.1i at all wavelengths. The dashed lines labelled NAS use this refractive index and a broader size distribution (see text), as in the NAS report[5]. The extinction coefficient is the sum of the scattering and absorption coefficients and $\tilde{\omega}$ is the ratio of the scattering and extinction coefficients. For $1-\tilde{\omega}$ just less than unity the extinction is thus dominated by absorption, whereas for $1-\tilde{\omega} = 0.5$ the absorption and scattering coefficients are equal.

Fig. 2. Downward shortwave flux at the surface (Wm^{-2}) for an atmosphere containing soot aerosols, as a function of the aerosol loading and geometric-mean radius r_g (μm). The solar zenith angle is 60°. The solid curves link the wavelength-integrated (broad-band) fluxes for the column densities listed in the inset table. The corresponding hemispheric loadings (in millions of tonnes-Mt) are also shown. The dashed curves link the fluxes obtained by scaling the values from band 8 of the scheme (λ = 0.52-0.57 μm) so that for clear-skies (curve 1) the wavelength-integrated fluxes are reproduced.

Fig. 3. Downward shortwave flux at the surface (Wm^{-2}) plotted against the aerosol column density (gm^{-2}), for three cases each with r_g = 0.1 μm. The labelling is the same as in Fig. 1. The solid lines indicate the broad-band fluxes and the dashed lines have the same meaning as in Fig. 2. On this type of plot, attenuation obeying a simple exponential law produces a straight line, which the dashed lines follow closely. The slope of the solid lines decreases with increasing column density, however, because at small pathlengths the slope is determined by the high attenuation at the shorter wavelengths, whereas at high pathlengths there is proportionally more radiation with longer wavelengths, for which the attenuation is weaker.

Fig. 4. Vertical profiles of heating rate for the same column densities as in Fig. 2 but using the NAS baseline aerosol properties[5]. In the clear-sky profile (curve 1) the tropospheric heating is from water vapour absorption and the stratospheric heating from ozone absorption. A component of the latter is due to absorption of the diffuse beam reflected back upwards from lower levels. The heating thus falls when the aerosol density increases as this beam is attenuated. The inset table lists the broad-band (left) and scaled-0.55 μm (right) values of the surface flux and the broad-band reflected flux at 100 km altitude.

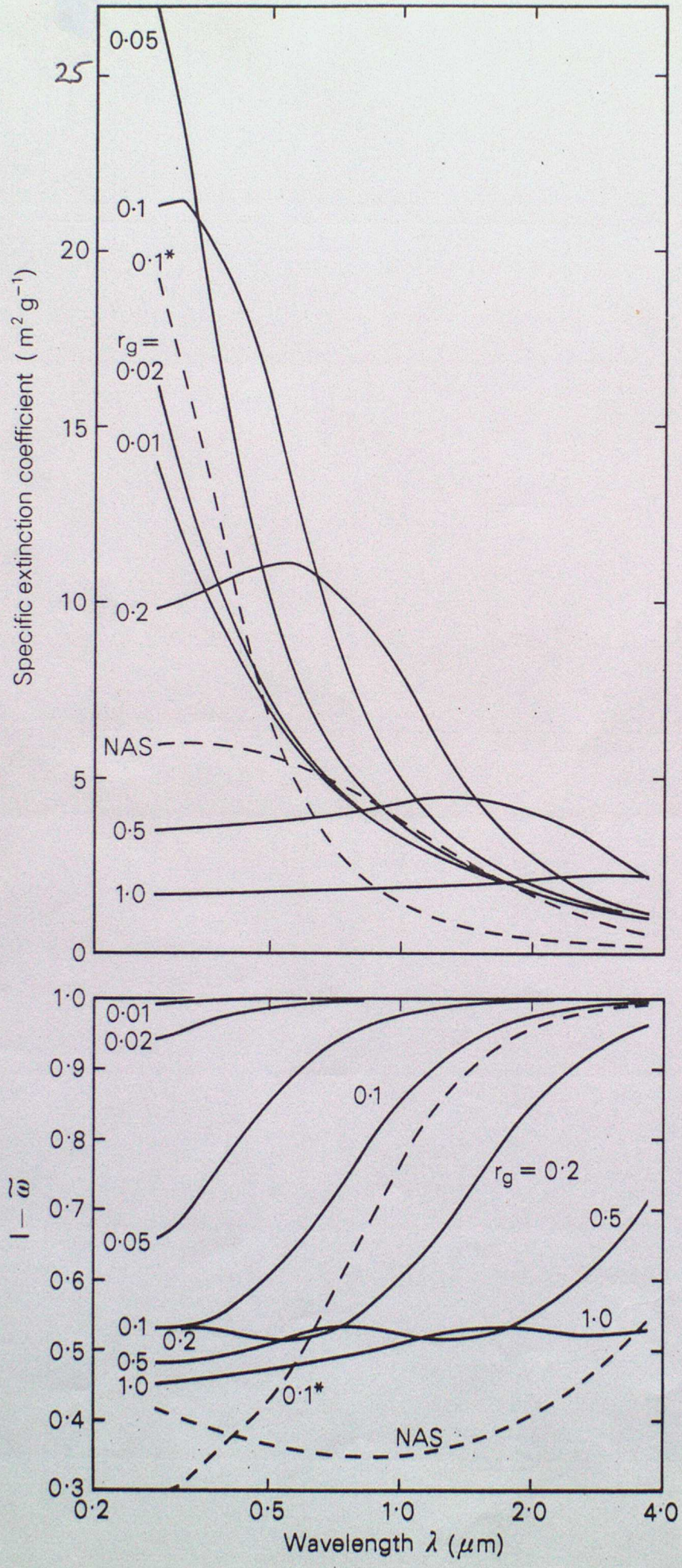
Specific extinction coefficient ($m^2 g^{-1}$)
25
20
15
10
5
0
0·05
0·1
0·1*
r_g =
0·02
0·01
0·2
NAS
0·5
1·0
1·0
0·9
0·8
0·7
0·6
0·5
0·4
0·3
1 − ϖ
0·01
0·02
0·1
0·05
r_g = 0·2
0·5
1·0
0·1
0·2
0·5
1·0
0·1*
NAS
0·2
0·5
1·0
2·0
4·0
Wavelength λ (μm)

Fig. 1

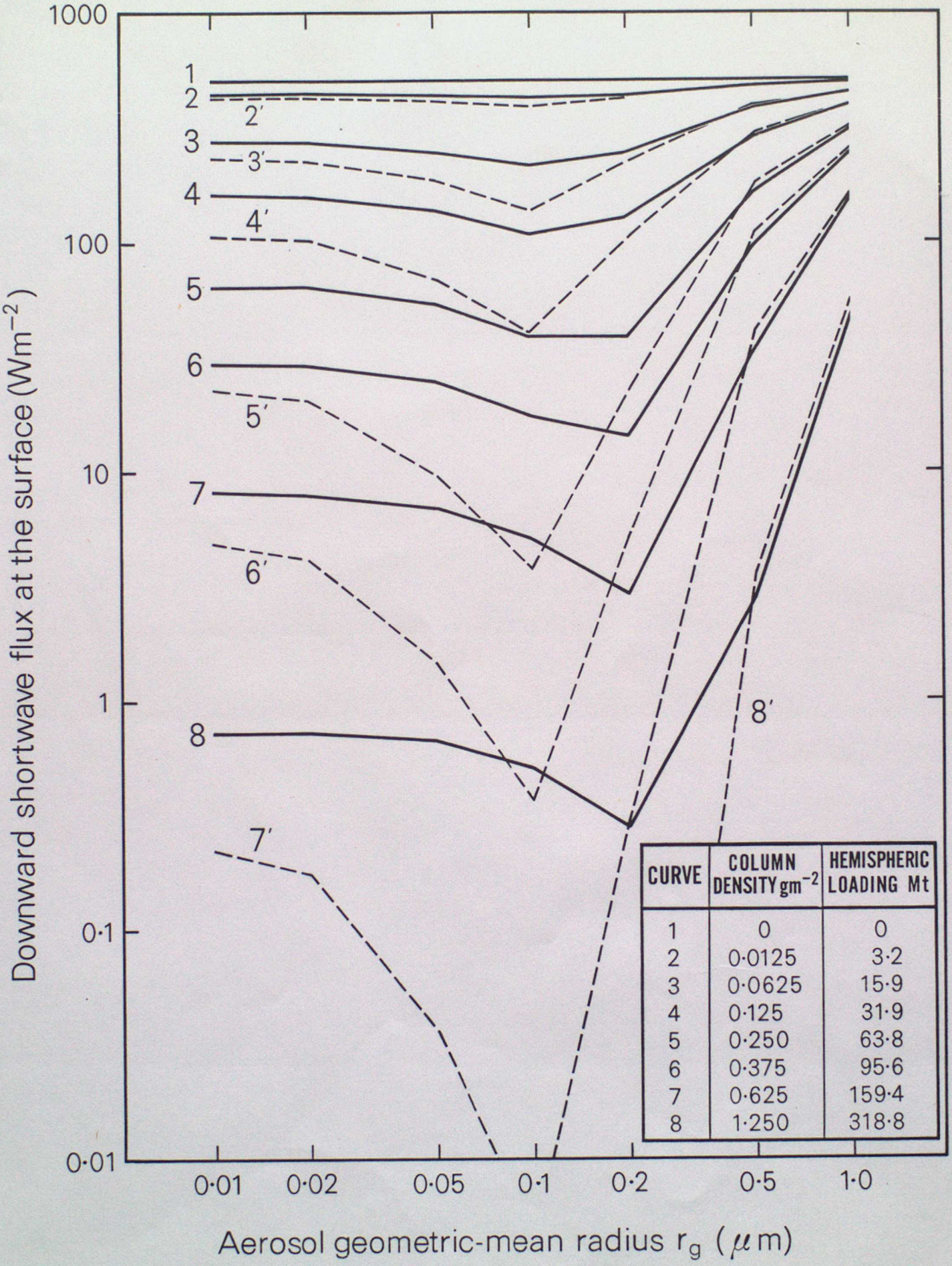

CURVE	COLUMN DENSITY gm^{-2}	HEMISPHERIC LOADING Mt
1	0	0
2	0·0125	3·2
3	0·0625	15·9
4	0·125	31·9
5	0·250	63·8
6	0·375	95·6
7	0·625	159·4
8	1·250	318·8

Fig. 2

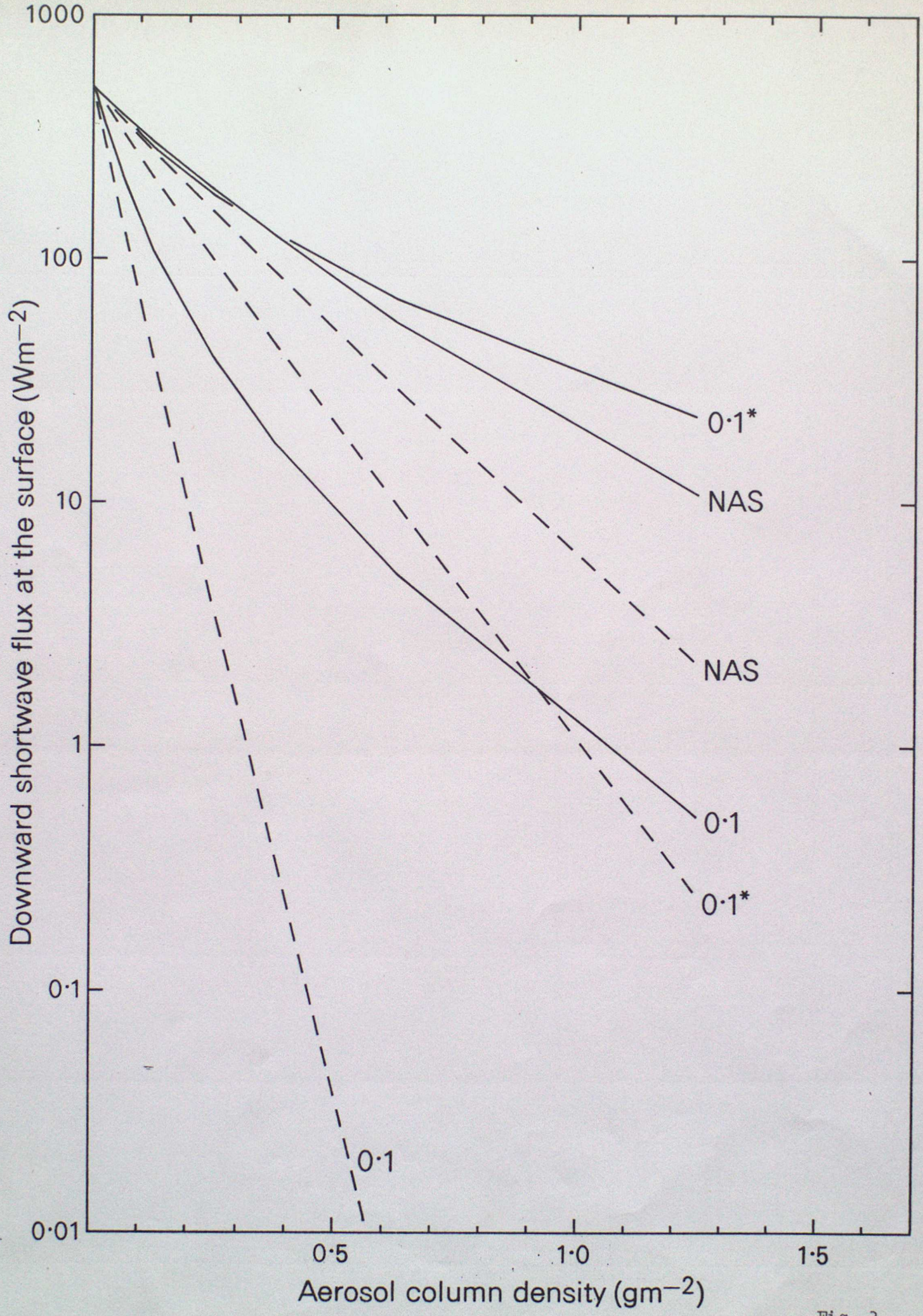
1000
100
10
1
0·1
0·01
Downward shortwave flux at the surface (Wm^{-2})
0·5
1·0
1·5
Aerosol column density (gm^{-2})
0·1*
NAS
NAS
0·1
0·1*
0·1

Fig. 3

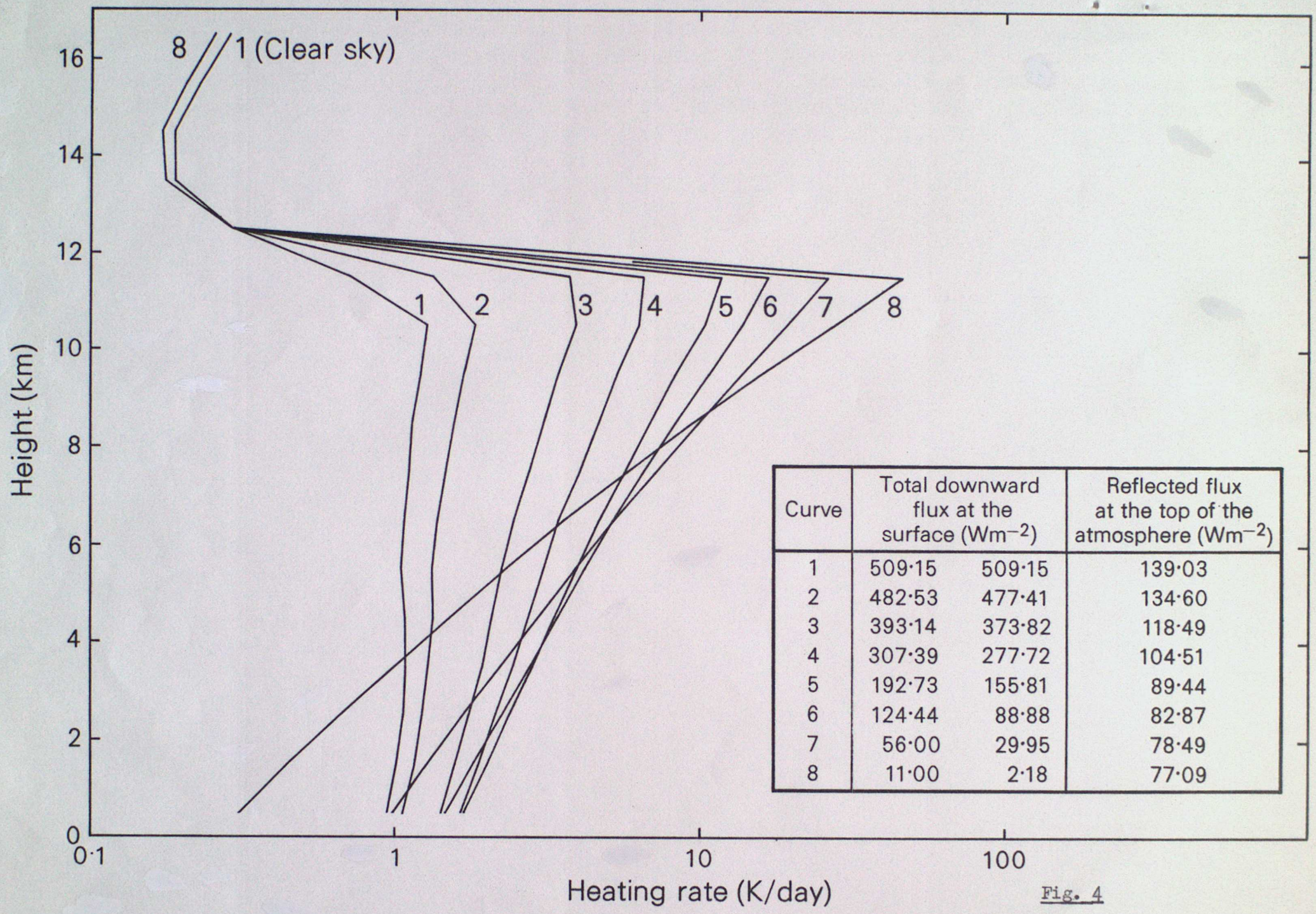

Curve	Total downward flux at the surface (Wm^{-2})		Reflected flux at the top of the atmosphere (Wm^{-2})
1	509·15	509·15	139·03
2	482·53	477·41	134·60
3	393·14	373·82	118·49
4	307·39	277·72	104·51
5	192·73	155·81	89·44
6	124·44	88·88	82·87
7	56·00	29·95	78·49
8	11·00	2·18	77·09

Fig. 4

DYNAMICAL CLIMATOLOGY TECHNICAL NOTES

DCTN 1	June 1984	A scheme for incorporating the thermodynamic sea-ice model into a coupled ocean-atmosphere model. C Gordon and M Bottomley
DCTN 2	Sept 1984	The parametrization of the upper ocean mixed layer in coupled ocean/atmosphere models. C Gordon and M Bottomley
DCTN 3	Sept 1984	The response of a simple thermodynamic sea-ice model to GCM forcing appropriate for perennial sea-ice. M Bottomley
DCTN 4	Sept 1984	Potential vorticity in the stratosphere derived using data from satellites. S A Clough, N S Grahame and A O'Neill
DCTN 5	Sept 1984	Simulation of the seasonal cycle of SST using globally specified climatological data to force simple ocean models. N S Grahame
DCTN 6	Sept 1984	Development of an improved GCM radiation scheme. A Slingo and R C Wilderspin
DCTN 7	Sept 1984	On the specification of surface fluxes in coupled atmosphere/ocean general circulation models. J F B Mitchell, C A Wilson and C M Price
DCTN 8	Sept 1984	A survey of possible repercussions of the Soviet river reversal programme on Arctic sea-ice. H Cattle
DCTN 9	Oct 1984	A study of a strong stratospheric warming during January 1982 T D A Fairlie
DCTN 10	Nov 1984	An intercomparison of the Met O 11 N45 model and the Met O 20 11-level model on the Cyber 205 J F Dyson
DCTN 11	Nov 1984	Simulation of observed time series of temperature and precipitation over eastern England. D N Reed
DCTN 12	Nov 1984	Forecasts and analyses of the onset of the Southwest monsoon. R Kershaw
DCTN 13	Nov 1984	On modelling the effects of CO_2 on climate. J F B Mitchell
DCTN 14	Dec 1984	Development of a revised longwave radiation scheme for an atmospheric general circulation model. A Slingo and R C Wilderspin
DCTN 15	Jan 1985	Rossby wavetrains in the stratosphere forced by localised disturbances in the troposphere. C J Marks (Oxford), A O'Neill and V D Pope

DYNAMICAL CLIMATOLOGY TECHNICAL NOTES

DCTN 16	Jan 1985	Observing system experiments using the Meteorological Office's 15-level model. R A Bromley
DCTN 17	Feb 1985	Atmospheric general circulation simulation of the climate of the Mediterranean region. H Cattle
DCTN 18	Feb 1985	Diurnal variation and cloud in a general circulation model. C A Wilson and J F B Mitchell
DCTN 19	Feb 1985	The sensitivity of the Saharan region in a general circulation model. W M Cunnington and P R Rowntree
DCTN 20	Mar 1985	The impact of aircraft observations on analyses and forecasts from the operational 15-level model. B R Barwell
DCTN 21	Mar 1985	Non-linear effects on heat-induced circulation of the tropical atmosphere. A E Gill and P J Phlips
DCTN 22	Apr 1985	Simulation of cloudiness with the U.K. Meteorological Office 11-layer AGCM. A Slingo and R C Wilderspin
DCTN 23	Apr 1985	An integrated approach to the representation of cloud processes.
DCTN 24	May 1985	Nuclear Winter: Calculations of the shortwave radiative effects of soot aerosols. A Slingo and P Goldsmith